Supporting Information

Chiarlone et al. 10.1073/pnas.1400988111

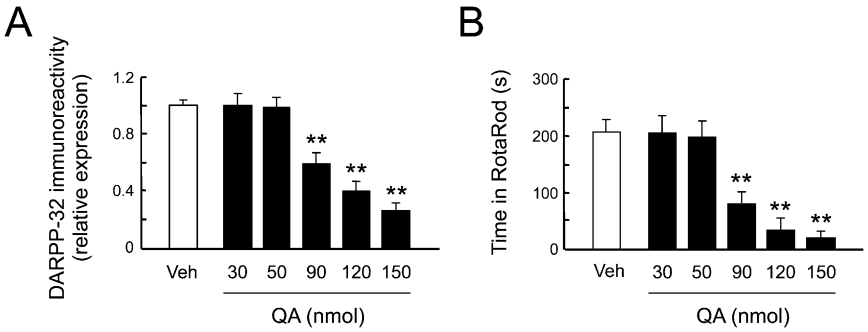

Fig. S1. Dose-dependent striatal damage induced by focal quinolinic acid (QA) injection. (*A* and *B*) WT (C57BL/6N) mice were injected intrastriatally with vehicle (Veh) or the indicated doses of QA (in 1 μL PBS solution, unilaterally; $n = 6–8$ animals per group). RotaRod performance was evaluated during the following 3 d (*B*), and animals were killed the day after for determination of dopamine- and cAMP-regulated phosphoprotein of 32 kDa (DARPP-32) immunoreactivity in the dorsolateral striatum (*A*). Data expressed as relative values vs. vehicle-treated group (**$P < 0.01$ vs. vehicle-treated group).

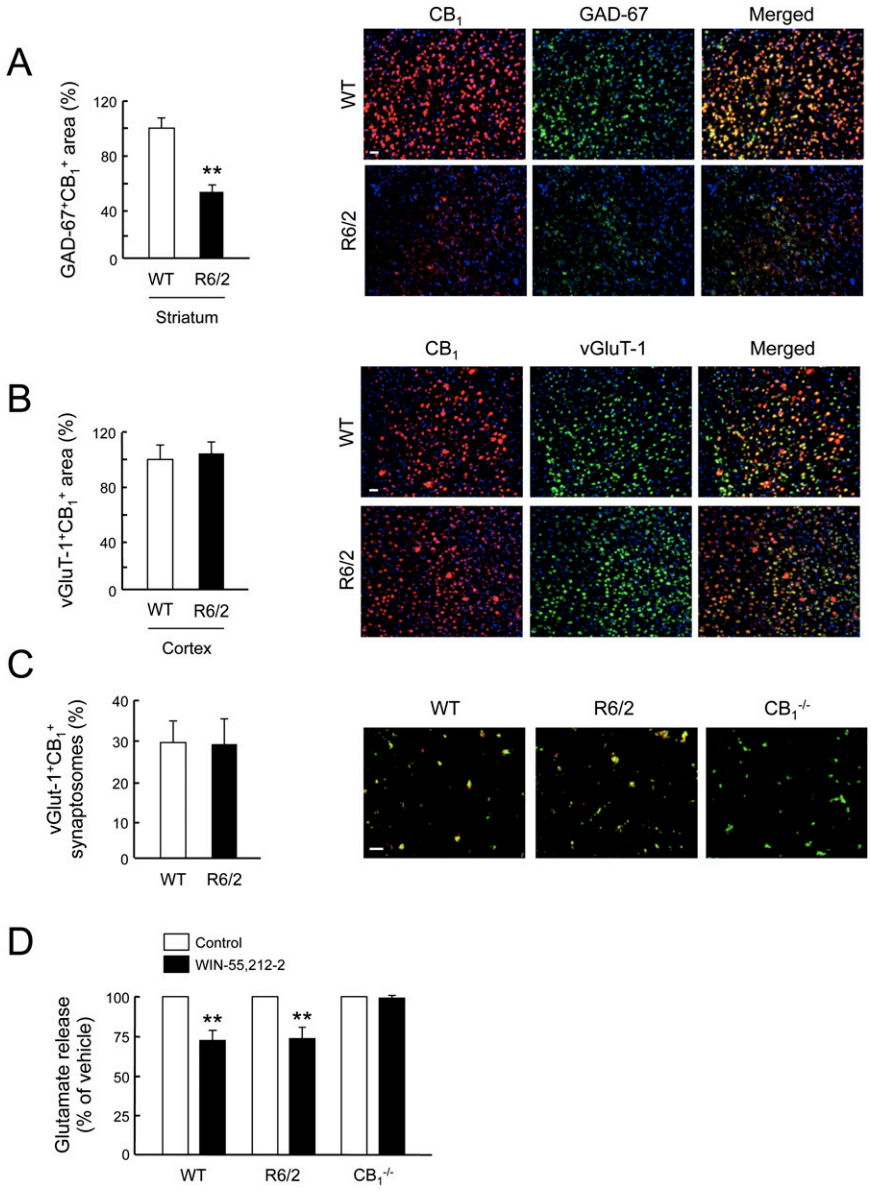

Fig. S2. CB_1 cannabinoid receptors are preserved on glutamatergic terminals in the striatum of symptomatic R6/2 mice. (*A* and *B*) Brain sections were obtained from 10-wk-old R6/2 mice and WT littermates. The coexpression of CB_1 and glutamic acid decarboxylase of 67 kDa (GAD-67) mRNAs in the dorsolateral striatum (*A*) or CB_1 and vesicular glutamate transporter-1 (vGluT-1) mRNAs in the deep motor cortex (*B*) was quantified by in situ hybridization. Data are given as area of coexpression relative to total cells recorded (DAPI staining; $n = 4$ animals per group; $^{**}P < 0.01$ vs. corresponding WT group). (Scale bars, 50 μm.) (*C*) Striatal synaptosomes were isolated from 10-wk-old R6/2 mice and WT littermates. CB_1-expressing glutamatergic synaptosomes ($Bassoon^+vGluT\text{-}1^+CB_1^+$ structures) were counted and given as percentage of total synaptosomes ($Bassoon^+$ structures). Data correspond to three pools of R6/2 or WT mouse-derived synaptosomes, each of which was obtained by combining the striata of four R6/2 or WT mice. Representative images are shown (CB_1, red; vGluT-1, green; Bassoon, blue, omitted for clarity). Striatal synaptosomes from $CB_1^{-/-}$ mice were used as control of CB_1 staining. (Scale bar, 20 μm.) (*D*) CB_1 receptors preserved on glutamatergic terminals in the striatum of symptomatic R6/2 mice are functionally active. Effect of the cannabinoid receptor agonist WIN-55,212-2 (5 μM) on 30 mM KCl-evoked glutamate release in striatal synaptosomes from 10-wk-old R6/2 mice and WT littermates. Striatal synaptosomes from $CB_1^{-/-}$ mice were used as control of WIN-55,212-2 action ($^{**}P < 0.01$ vs. corresponding control group).

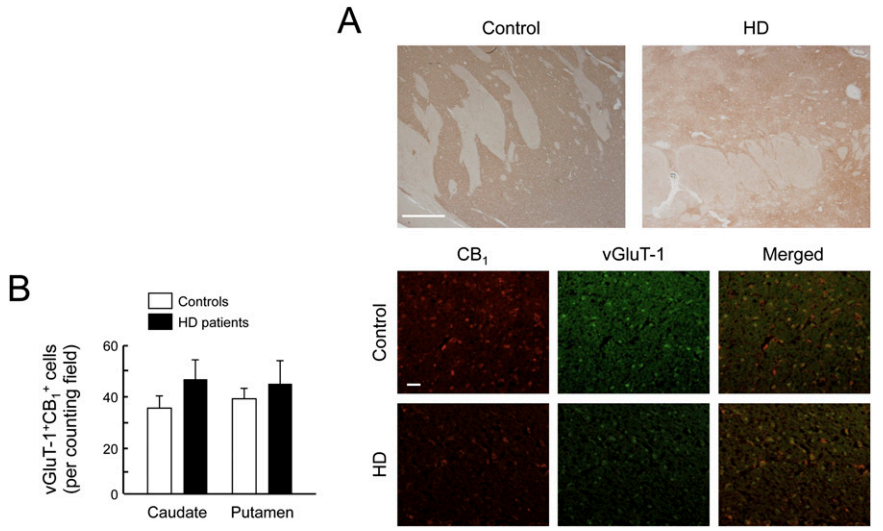

Fig. S3. CB_1 cannabinoid receptors are preserved on glutamatergic terminals in postmortem caudate-putamen specimens of patients with Huntington disease (HD). (*A*) Representative low-magnification immunohistochemistry images of CB_1 receptor staining in a control subject and a patient with HD. (Scale bar, 800 μm.) (*B*) Immunofluorescence analysis of CB_1/vGluT-1 coexpression in control subjects ($n = 5$) and patients with HD (grades 3–4; $n = 7$). Representative images are shown (DAPI, blue, omitted for clarity). (Scale bar, 50 μm.)

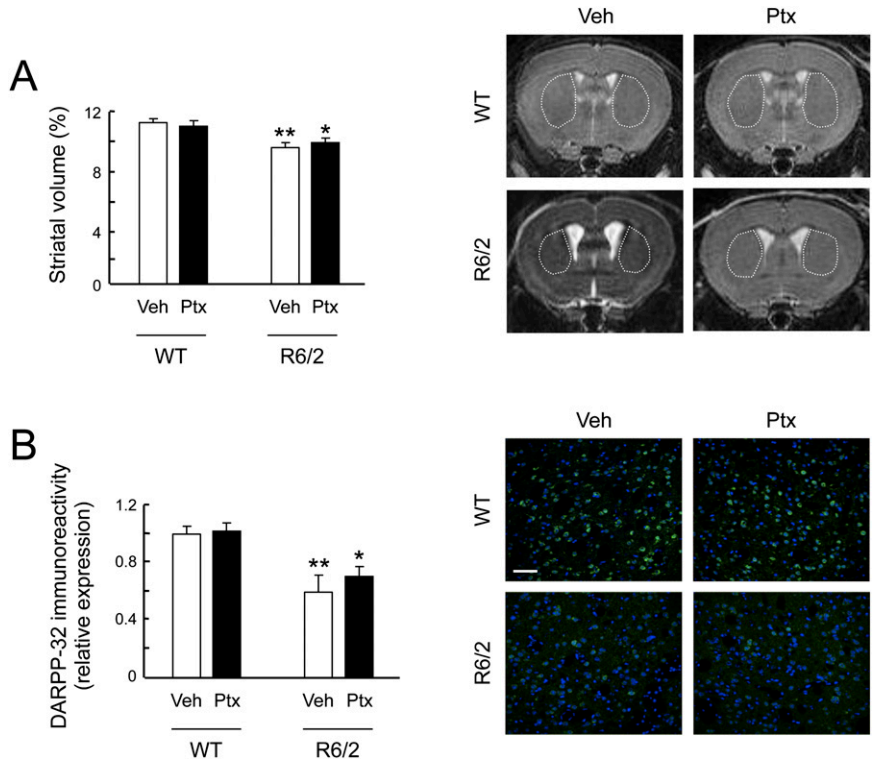

Fig. S4. Pharmacological blockade of $GABA_A$ receptors does not prevent HD-like striatal neurodegeneration in symptomatic R6/2 mice. (*A* and *B*) R6/2 mice and WT littermates were treated i.p. with vehicle (Veh) or picrotoxin (Ptx; 0.3 mg/kg body weight per day) from week 8 to week 12 of age. (*A*) Striatal volume (percentage of total brain volume). Representative MRI images are shown. The striata are outlined. (*B*) DARPP-32 immunoreactivity in the dorsolateral striatum (relative values from the vehicle-treated WT group). Representative images are shown (DARPP-32, green; Hoechst 33342, blue). (Scale bar, 50 μm.) Data in *A* and *B* correspond to 12-wk-old mice at the end of the treatments ($n = 6$–8 animals per group; $^*P < 0.05$ and $^{**}P < 0.01$ vs. corresponding WT group).

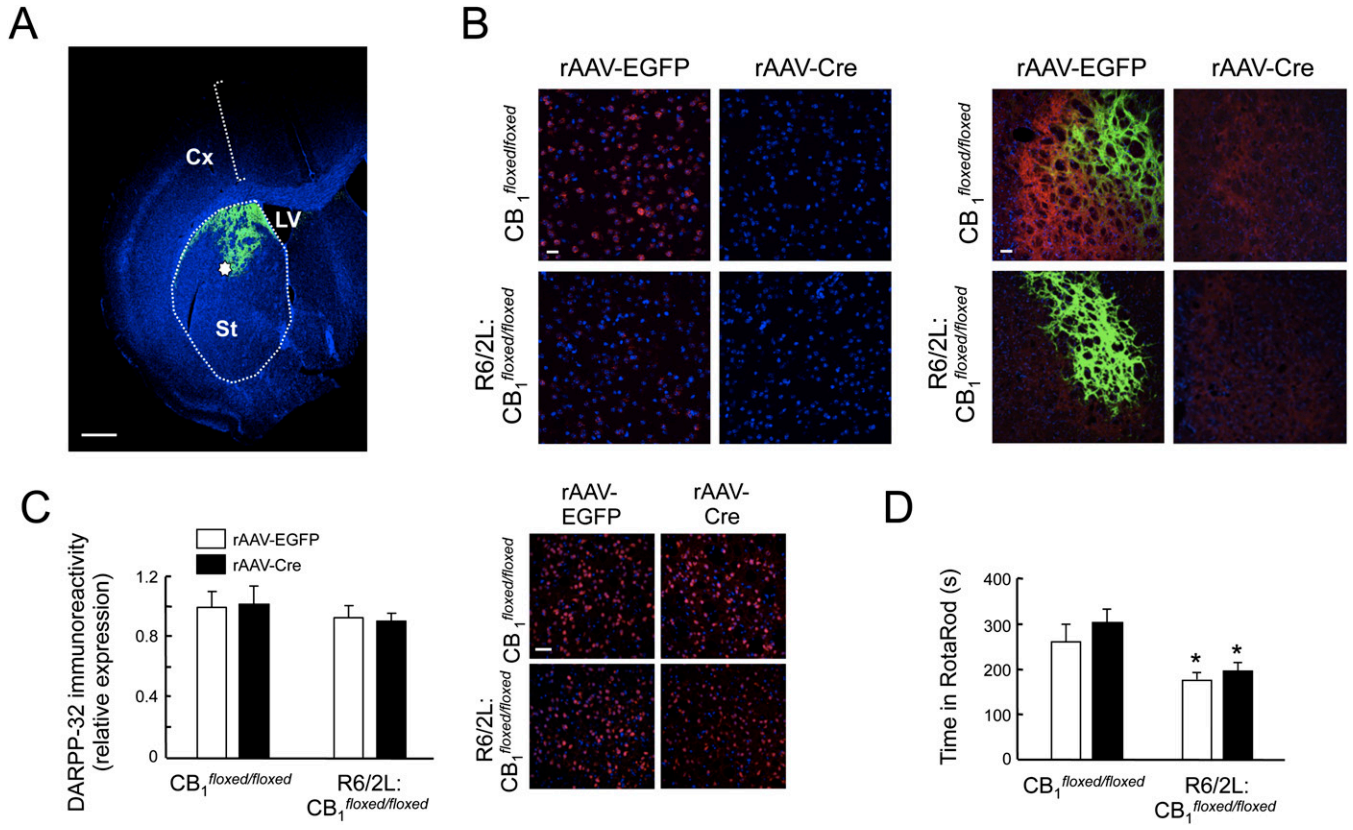

Fig. S5. Cre recombinase-driven deletion of CB_1 cannabinoid receptors in the dorsolateral striatum does not affect HD-like neurodegeneration. (*A–D*) Four-week-old R6/2L:$CB_1^{floxed/floxed}$ mice and $CB_1^{floxed/floxed}$ littermates were injected stereotactically into the dorsolateral striatum with a recombinant adenoassociated virus (rAAV) encoding Cre recombinase (or EGFP) under the control of the calcium/calmodulin-dependent protein kinase II-α (CaMKIIα) promoter (n = 8–12 animals per group). At week 20 of age, RotaRod performance was evaluated, and animals were killed the day after for histological analyses. (*A*) Example of a brain hemisphere injected with rAAV–calcium/calmodulin-dependent protein kinase II-α promoter–EGFP (EGFP, green; DAPI, blue). Cx, cortex; LV, lateral ventricle; St, striatum (*approximate site of injection). (Scale bar, 500 μm.) (*B*) (*Left*) Representative images of CB_1 receptor mRNA in situ hybridization in the dorsolateral striatum (CB_1, red; DAPI, blue). Note the Cre-mediated reduction of CB_1 mRNA expression. (Scale bar, 50 μm.) (*Right*) Representative images of CB_1 receptor immunostaining in the globus pallidus (a major projecting area of medium-sized spiny neurons; CB_1, red; EGFP, green; DAPI, blue). Note the Cre-mediated reduction of CB_1 protein expression. (Scale bar, 50 μm.) (*C*) DARPP-32 immunoreactivity in the dorsolateral striatum (relative values vs. corresponding rAAV-EGFP–injected $CB_1^{floxed/floxed}$ group). Representative images of DARPP-32 staining are shown (DARPP-32, red; DAPI, blue). (Scale bar, 50 μm.) (*D*) RotaRod performance (i.e., time to fall). (*$P < 0.05$ vs. corresponding $CB_1^{floxed/floxed}$ group.)